Participation of the Amino-Terminal Domain in the Self-Association of the Full-Length Yeast TATA Binding Protein†

Margaret A. Daugherty,‡ Michael Brenowitz,§ and Michael G. Fried*,‡

Department of Biochemistry and Molecular Biology, The Pennsylvania State University College of Medicine, Hershey, Pennsylvania 17033, and Department of Biochemistry, Albert Einstein College of Medicine, 1300 Morris Park Avenue, Bronx, New York 10461

Received October 19, 1999; Revised Manuscript Received February 22, 2000

ABSTRACT: The association of monomeric TATA binding protein with promoter DNA is an essential first step in many current models of eukaryotic transcription initiation. This step is followed by others in which additional transcription factors, and finally RNA polymerase, assemble at the promoter. Here we characterize the quaternary interactions of the *Saccharomyces cerevisiae* TATA-binding protein (yTBP), in the absence of other proteins or DNA. The data reveal a robust pattern in which yTBP monomers equilibrate with tetramers and octamers over a broad span of temperatures (4 °C ≤ T ≤ 37 °C) and salt concentrations (60 mM ≤ [KCl] ≤ 1 M), that includes the physiological range. Association is highly cooperative, with octamer formation favored by ∼9 kcal/mol over tetramer formation. Changes in association constant with [KCl] are consistent with an assembly-linked release of ions at low salt and an assembly-linked uptake of ions at high salt, for both monomer ⇄ tetramer and tetramer ⇄ octamer reaction steps. Fluorescence emission spectra and steady-state anisotropies reveal that the amino-terminal domain changes conformation and dynamics at both association steps and that the polarity of the environment near tryptophan 26 is sensitive to changes in [KCl] in the monomeric and tetrameric states but not the octameric state. These results are consistent with a [salt]-dependent change in the assembly mechanism near 300 mM KCl and suggest that the amino-terminal domain may modulate the self-association of the full-length protein. TBP self-association may regulate many of its cellular functions, including transit of the nuclear membrane and participation in transcription initiation.

The TATA binding protein (TBP)[1] plays central roles in the transcription initiation pathways of the three major eukaryotic RNA polymerases (polymerase I, polymerase II, and polymerase III) (*1, 2*). At TATA-containing promoters, protein complexes containing TBP and *T*BP-*a*ssociated protein *f*actors (TAFs) bind the DNA (*3, 4*), providing nucleation sites for the assembly of general transcription factors and the cognate RNA polymerase (*5*−*7*). At promoters that lack the TATA sequence, TBP−TAF complexes mediate the assembly of promoter-specific transcription factors, possibly without binding DNA (*8*−*12*).

The currently available evidence suggests that the form of TBP that functions in transcription initiation is the monomer. TBP binds TATA-sequence DNA as a monomer (*13*−*18*) and interacts with TAFs and general transcription factors as a monomer (*19*−*23*). On the other hand, TBP is capable of self-association. Dimers, tetramers, octamers, and higher oligomers have been previously reported (*24*−*29*). Although direct evidence of roles for these oligomeric TBP species has yet to be found, monomer−oligomer equilibria may influence the concentration of free monomer that is available for transcription regulatory functions in vivo (*26, 30*).

Little is known about the mechanism(s) of TBP self-association in solution. Crystal structures of the C-terminal domain of TBP from *Saccharomyces cerevisiae* and the full-length *Arabidopsis thaliana* TBP-2, which has a vestigial (18 residue) amino terminal domain, reveal highly similar, saddle-shaped molecules of ∼180 amino acid residues. The convex TAF and transcription factor-binding surfaces are rich in hydrophilic residues while the concave DNA-binding faces are rich in hydrophobic ones (*13*−*15, 24, 25, 31*). In the absence of DNA, both proteins crystallize as dimers, stabilized by extensive contacts between the concave surfaces (*24, 25, 31*). It has been suggested that similar interactions take place in solution (*16, 24*−*26*). Consistent with this notion, evidence has been presented that TBPs from *Homo sapiens* and *Pyrococcus woesei* form dimers in solution (*26, 32*). However, other association patterns have been found for TBPs from mouse, human, and yeast (*16, 27*−*29, 33*). In the case of yeast TBP, monomers were found to be in equilibrium with tetrameric and octameric species at 30 °C, over a wide range of KCl concentrations (*29*).

The variety of association patterns observed among different species and under different experimental conditions

† Supported by NIH GM48517 to M.G.F., a Four Diamonds Fund Postdoctoral Grant to M.A.D., and NIH GM39929 to M.B.

* Corresponding author. Telephone: (717) 531-5250. Fax: (717) 531-7072. E-mail: mfried@psu.edu.

‡ The Pennsylvania State University College of Medicine.

§ Albert Einstein College of Medicine.

[1] Abbreviations: TBP, TATA-binding protein; yTBP, the full-length TBP from *S. cerevisiae*; TAFs, TBP-associated factors.

10.1021/bi992423n CCC: $19.00
Published on Web 03/31/2000

raises a number of important questions including: Do solution variables qualitatively and/or quantitatively control the assembly of a given TBP molecule? What roles do the poorly conserved N-terminal and highly conserved C-terminal domains play in mediating the self-association pattern? How does self-association influence the functional DNA and protein interactions of TBP? Clearly, quantitative characterization of TBP self-association reactions is needed in order to answer these questions.

In this paper, we present a characterization of thermodynamic and fluorescence changes that accompany the individual steps of yeast TBP oligomerization. We show that yTBP associates to tetramers and octamers over a very wide range of solution conditions, that this association is highly cooperative, and that both reaction steps are strongly entropy-driven. Both the ion linkage and fluorescence results provide evidence of a monovalent ion concentration-dependent shift in the self-association mechanism. The fluorescence data are consistent with assembly mechanisms in which the amino-terminal domain undergoes significant changes in conformation and dynamics. Since the C-terminal domain of yeast TBP forms stable dimers (*25*), these results suggest that the nonconserved amino-terminal domain may play a role in modulating the self-association of the full-length protein.

EXPERIMENTAL PROCEDURES

Protein. TATA binding protein from the yeast *Saccharomyces cerevisiae* (yTBP) was purified as previously described (*17*, *34*) and was fully active in DNA binding as measured by footprinting and fluorescence (*18*, *35*) and sedimentation equilibrium methods (M. Daugherty, unpublished results). It was stored in small aliquots at −80 °C and dialyzed at 4 °C, just prior to centrifugation, against buffer containing 20 mM Hepes/KOH, pH 7.9, 1 mM EDTA, 1 mM DTT, and KCl at a final concentration of 60 mM, 120 mM, 300 mM, 600 mM, or 1 M. In experiments designed to test the effects of $MgCl_2$, glycerol, and the nonionic detergent NP-40 on association, buffer containing 120 mM KCl was supplemented with 4 mM $MgCl_2$, 5% (v/v) glycerol, or 0.025% (v/v) NP-40. Because the pK_a of Hepes is temperature-dependent (*36*), the pH ranged from 7.68 to 8.14 over the 4−37 °C temperature range of the experiments reported here. Although the pH dependence of self-assembly has not been rigorously investigated, DNA binding reactions (in which the free monomer concentration should be perturbed by changes in self-association) appear to be independent of pH over the pH range of 5.5−9.0 (*34*). Protein concentrations were determined spectrophotometrically, using $\epsilon_{280} = 12\,700\ M^{-1}\ cm^{-1}$ (*18*).

Analytical Ultracentrifugation. Sedimentation equilibrium experiments were performed using a Beckman Optima XL-A analytical ultracentrifuge fitted with an AN-60Ti rotor. Six-sector centerpieces were used, allowing 9 samples of varying protein and/or salt concentration to be analyzed simultaneously. Absorbance values were measured at 280 nm as a function of radial position. Approach to equilibrium was considered complete when replicate scans separated by ≥6 h were indistinguishable. To determine the temperature dependence of association equilibrium constants, data were collected at 16 000 and 24 000 rpm at each of seven temperatures (4, 10, 14, 20, 24, 30, and 37 °C). Samples were routinely subjected to SDS−polyacrylamide gel electrophoresis following ultracentrifugation. In no case was protein degradation detected by this means (data not shown).

Sedimentation equilibrium data were analyzed using homogeneous self-association models (*29*). For a system in which monomers, tetramers, and octamers are at equilibrium, the concentration of each species at radial position c_r is given by

$$c_r = c_M \exp \xi_M + (c_M)^4 K_{14} \exp \xi_T + (c_M)^8 K_{18} \exp \xi_O + \alpha \quad (1a)$$

Here the concentration of species i at the reference radius, r_o, is related to its absorbance by $c_{r_o,i} = A_{r_o,i}/\epsilon 1$, where ϵ is the extinction coefficient, and the parameter ξ_i is equal to $(\omega^2/2RT)M_i(1 - \bar{\nu}\rho)(r^2 - r_0^2)$, in which ω is the angular velocity, R is the gas constant in units of erg/mol-K, T is the temperature in Kelvin, M_i is the molecular weight of species i, $\bar{\nu}$ is the partial specific volume of species i, and ρ is the density of the solvent. The subscripts M, T, and O represent monomeric, tetrameric, and octameric species, respectively, and the concentrations of tetramer and octamer depend on that of monomer as described by the mass-action relations $[T] = K_{14}[M]^4$ and $[O] = K_{18}[M]^8$. The value of $\bar{\nu}$ was estimated from the amino acid composition of TBP by the method of Cohn (*37*) and corrected for temperature according to McRorie and Voelker (*38*). The values of $\bar{\nu}$ for TBP oligomers were taken to be equal to that of the monomeric protein. Similarly, the extinction coefficient of the TBP monomer was assumed to be unchanged by self-assembly (*29*). Buffer densities (ρ) were determined using a Mettler DA-300 density meter, operated at the measurement temperature. The baseline offset constant, α, is included to account for slight position-independent variations in the optical properties of individual samples and/or cell assemblies.

For a system in which monomers are in equilibrium with octamers, the distribution of protein at sedimentation equilibrium is governed by

$$c_r = c_M \exp \xi_M + (c_M)^8 K_{18} \exp \xi_O + \alpha \quad (1b)$$

Association constants were estimated by simultaneous least-squares fitting of eq 1 to multiple data sets ("global analysis") using the NONLIN[2] software running on a Macintosh computer (*39*). Typical analyses utilized four data sets, corresponding to two samples differing in nominal protein concentration, brought to equilibrium at two rotor speeds.

Fluorescence Spectroscopy. Measurements were made using an Aminco-Bowman 2 fluorometer. Samples were brought to equilibrium at 30 °C in 20 mM Hepes/KOH, pH 7.9, 1 mM EDTA, and 1 mM DTT buffer containing 60, 300, or 600 mM KCl. Emission spectra were collected using an excitation wavelength of 293 nm. Five replicate scans were averaged, and the independently-measured Raman spectrum of H_2O was subtracted. Fluorescence anisotropy values were obtained using excitation and emission wavelengths of 293 and 338 nm, respectively. The sample was irradiated with vertically polarized light, and anisotropy was

[2] NONLIN for the Macintosh was obtained from the website http://bioc02.uthscsa.edu/.biochem/xla2.html.

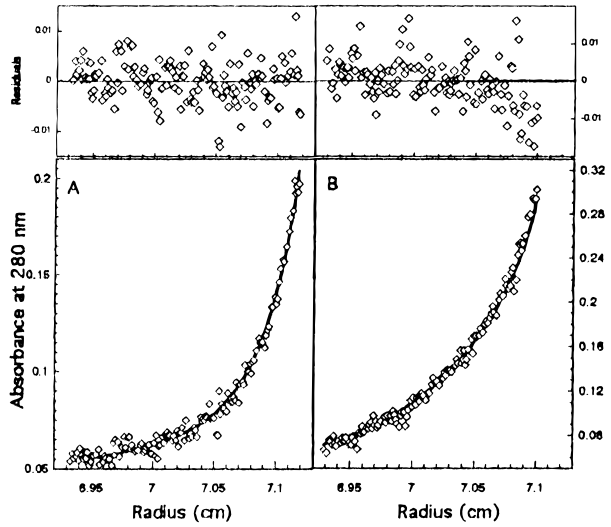

FIGURE 1: Representative sedimentation equilibrium data. (A) Yeast TBP centrifuged to equilibrium at 16 000 rpm and 4 °C in buffer containing 60 mM KCl. The solid line represents the global fit of eq 1a to the entire ensemble of data sets obtained at 4 °C and 60 mM KCl as described in Experimental Procedures. (B) TBP centrifuged to equilibrium at 16 000 rpm and 30 °C in buffer containing 600 mM KCl. The solid line represents the global fit of eq 1a to the ensemble of data sets obtained at 30 °C and 600 mM KCl as described in Experimental Procedures. In both cases, the curve-fitting residuals (upper panels) are small and appear to be randomly distributed, demonstrating that the monomer−tetramer−octamer model is consistent with the mass distribution of TBP present in these samples.

calculated from the ratio of polarized emission intensities shown here:

$$r = \frac{I_V - GI_H}{I_V + 2GI_H} \quad (2)$$

Here I_V and I_H represent the vertically polarized and horizontally polarized emission intensities, and $G = S_V/S_H$, the ratio of detector sensitivity to vertically and horizontally polarized light (*40*). In all cases, three or more measurements were averaged.

RESULTS

Cooperative Monomer−Tetramer−Octamer Association Is Observed over a Wide Range of Conditions. Equilibrium analytical ultracentrifugation was used to investigate the self-assembly of full-length yeast TBP at five KCl concentrations (60 mM, 120 mM, 300 mM, 600 mM, and 1 M KCl) and seven temperatures (4, 10, 14, 20, 24, 30, and 37 °C). Representative data sets obtained under different salt and temperature conditions are shown in Figure 1. Superimposed on these data are theoretical curves showing the global fit of eq 1a to the entire data ensemble obtained under each solution condition. The small, uniformly distributed residuals indicate that the monomer ⇄ tetramer ⇄ octamer model is consistent with these data sets. In all cases, the use of expressions that included terms for *dimeric* TBP resulted in large, nonrandom residuals and significantly higher values for the square root of the variance than did fits to expressions containing all terms but those for the dimer (results not shown; cf. ref *29*). These results argue against the presence of *detectable* amounts of dimeric TBP in our equilibrium

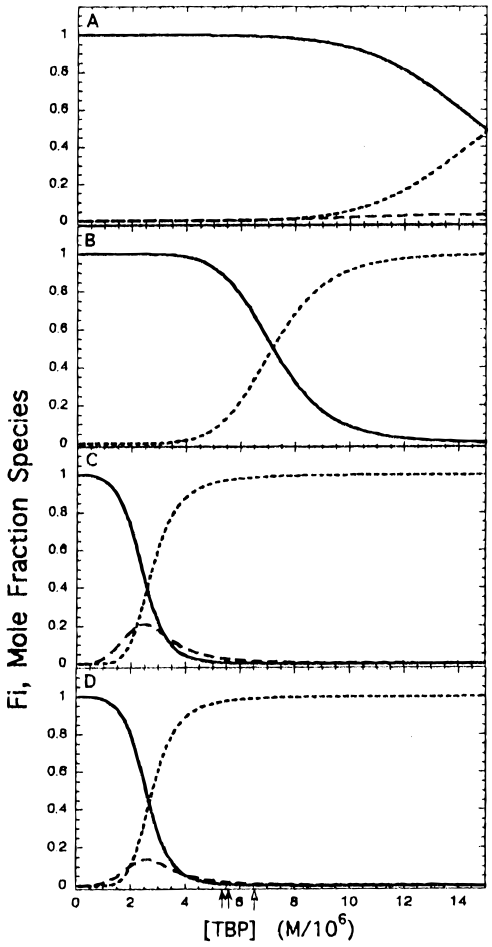

FIGURE 2: Dependence of the mole fractions of monomeric, tetrameric, and octameric species on total TBP concentration. The mole fractions of monomers (solid line), tetramers (dashed line), and octamers (dotted line) were calculated using association constants obtained by global analysis of data for TBP solutions sedimented to equilibrium in buffer containing 120 mM KCl at various temperatures: (A) 4, (B) 10, (C) 24, and (D) 30 °C, In panel D, the open-point arrowhead represents the concentration of TBP estimated in the yeast nucleus (*29*), and the closed-point arrowheads represent the estimated concentration range of TBP in the yeast nucleus assuming that each gene in the yeast genome has a uniquely associated TBP (see text).

mixtures. The monomer ⇄ tetramer ⇄ octamer model was compatible with experimental data obtained over a wide range of TBP concentrations (∼800 nM ≤ [TBP] ≤ ∼160 μM), KCl concentrations (60 mM ≤ [KCl] ≤ 1 M), and temperatures (4 °C ≤ T ≤ 37 °C). This consistency argues that the monomer ⇄ tetramer ⇄ octamer association pattern is a "native" mode of oligomerization and not an artifact of a single choice of solution conditions.

The tetrameric species is a minor component under all conditions examined, typically not exceeding a mole fraction of 0.2 (Figure 2). In a few cases, the concentrations of tetramer that fit the data were close to zero; under these conditions, a satisfactory fit was also obtained with a monomer−octamer association model (eq 1b). In general, this result was obtained at low temperatures, suggesting that the tetrameric state is disfavored relative to monomer and octamer under these conditions. However, under most conditions, the concentrations of monomers, tetramers, and octamers could be determined with confidence, and the

Table 1: Thermodynamic Parameters for TBP Oligomerization[a]

A: Monomer ⇄ Tetramer Equilibrium

[KCl] (mM)	$\Delta G^\circ_{303.15}$ (kcal/mol)	$\Delta H^\circ_{303.15}$ (kcal/mol)	$T\Delta S^\circ_{303.15}$ (kcal/mol)
60	−24.2 ± 0.8	22.1 ± 34.6	46.3 ± 34.7
120	−22.7 ± 0.6	44.7 ± 8.9	67.4 ± 9.1
300	−20.8 ± 0.4	74.7 ± 18.0	95.5± 18.0
600	−22.7 ± 0.9	57.4 ± 22.1	79.7 ± 22.4
1000	−22.1 ± 0.6	28.0 ± 26.7	50.1 ± 26.7

B: Tetramer ⇄ Octamer Equilibrium

[KCl] (mM)	$\Delta G^\circ_{303.15}$ (kcal/mol)	$\Delta H^\circ_{303.15}$ (kcal/mol)	$T\Delta S^\circ_{303.15}$ (kcal/mol)
60	−33.1 ± 1.5	−8.2 ± 60.4	24.9 ± 60.4
120	−31.7 ± 1.0	35.4 ±11.8	67.1 ± 12.5
300	−29.5 ± 0.6	60.0 ± 29.7	89.5 ± 29.7
600	−31.4 ± 1.1	35.0 ± 32.1	66.4 ± 32.6
1000	−31.9 ± 0.7	48.0 ± 35.1	79.9 ± 35.1

C: Monomer ⇄ Octamer Equilibrium

[KCl] (mM)	$\Delta G^\circ_{303.15}$ (kcal/mol)	$\Delta H^\circ_{303.15}$ (kcal/mol)	$T\Delta S^\circ_{303.15}$ (kcal/mol)
60	−57.2 ± 1.2	14.5 ± 47.7	71.7 ± 47.7
120	−54.4 ± 0.7	55.8 ± 30.1	110.2 ± 30.1
300	−50.4 ± 0.4	134.0 ± 19.5	184.4 ± 19.5
600	−53.7 ± 0.6	83.9 ± 22.9	140.6 ± 22.9
1000	−53.4 ± 0.4	77.1 ± 16.0	130.5 ± 16.0

D: Values of ΔC_p for Assembly Steps

[KCl] (mM)	$\Delta C^\circ_{p,1-4}$ (kcal/mol-K)	$\Delta C^\circ_{p,4-8}$ (kcal/mol-K)	$\Delta C^\circ_{p,1-8}$ (kcal/mol-K)
60	0.2 ± 2.7	−2.4 ± 4.6	−2.2 ± 3.6
120	nd	nd	−1.8 ± 2.2
300	3.3 ± 1.3	1.5 ± 2.0	4.6 ± 1.2
600	nd	nd	−1.0 ± 1.5
1000	−0.2 ± 2.8	−0.6 ± 3.6	0.1 ± 1.2

[a] Evaluated at the reference temperature $\theta = 303.15$ K (30 °C). nd, not determinable.

assembly of tetramers into octamers was favored by ~9 kcal/mol over the assembly of monomers into tetramers [(*29*); see also Table 1]. This cooperative effect increases the mole fraction of TBP sequestered in the octameric state.

The buffers used in transcription assays often contain components that are thought to enhance DNA binding and/or transcription activity. One such buffer is 20 mM Tris/acetate (pH 7.5), 5% glycerol, 75 mM potassium glutamate, 4 mM spermidine, 0.1 mM EDTA, 4 mM $MgCl_2$, 13 μM poly(dG-dC), 0.01% NP-40, and 5 μg/mL bovine serum albumin (*41*). It is not currently known what effect these components have on the conformational and association equilibria of yeast TBP. To address this issue, we tested the effects of glycerol (5% v/v), $MgCl_2$ (4 mM), and NP-40 (0.025% v/v) singly and in combination on TBP self-association under otherwise standard buffer conditions (20 mM Hepes/KOH, pH 7.9, 1 mM EDTA, 1 mM DTT, and 120 mM KCl). Neither the inclusion of glycerol nor $MgCl_2$ caused the pattern of association to deviate from monomer−tetramer−octamer. Moreover, the free energy differences for formation of tetramer from monomer and octamer from tetramer in the presence of 5% glycerol or 4 mM $MgCl_2$ were the same, within error, as those found in the absence of these reagents (data not shown). In contrast, the inclusion of a low concentration of NP-40 resulted in the formation of high molecular weight ($M_W = 322\,000 \pm 82\,000$) species. This weight-average molecular weight is roughly equal to that of 12 monomer units. These results indicate that the absence of $MgCl_2$ and glycerol from our standard buffers has no qualitative or quantitative effect on the species distributions of full-length yeast TBP. In addition, they indicate that the association equilibria of TBP are sensitive to detergent and open to question the physical state(s) of the protein in samples that contain even low concentrations of surfactant.

Thermodynamics of Oligomerization. At any temperature the changes in standard free energy, enthalpy, and entropy that accompany oligomerization are described by

$$\Delta G^\circ = \Delta H^\circ - T\Delta S^\circ \quad (3)$$

A deviation of ΔG° from a linear dependence on temperature can be expressed as a nonzero standard heat capacity difference ($\Delta C^\circ_{p,\theta}$) that contributes to enthalpy and entropy differences as shown here:

$$\Delta H^\circ = \Delta H^\circ_\theta - \Delta C^\circ_{p,\theta}(T - \theta) \quad (4a)$$

$$\Delta S^\circ = \Delta S^\circ_\theta - \Delta C^\circ_{p,\theta} \ln\left(\frac{T}{\theta}\right) \quad (4b)$$

Here, θ is a reference temperature, and ΔS°_θ and ΔH°_θ are the enthalpy and entropy differences at that temperature. Substituting eqs 4a and 4b into eq 3 gives an expression for the temperature dependence of the association constant (*42*):

$$R \ln K_{assoc} = -\frac{\Delta G^\circ_\theta}{\theta} + \Delta H^\circ_\theta\left(\frac{1}{\theta} - \frac{1}{T}\right) + \Delta C^\circ_{p,\theta}\left(\frac{\theta}{T} - 1 + \ln\left(\frac{T}{\theta}\right)\right) \quad (5)$$

The dependence of $R \ln K_{assoc}$ on temperature for representative monomer−tetramer, tetramer−octamer, and monomer−octamer association reactions is shown in Figure 3. The smooth curves are fits of eq 5 to the data, using $\theta = 303.15$ K (30 °C) as the reference temperature. We chose $\theta = 30$ °C because this is near the optimal growth temperature for *S. cerevisiae*. The departures from linearity that are evident in these graphs indicate nonzero values of $\Delta C^\circ_{p,\theta}$. Values of ΔG°_θ, ΔH°_θ, and $\Delta C^\circ_{p,\theta}$ obtained as fitting parameters using eq 5 and values of ΔS°_θ obtained by difference are presented in Table 1.

At all salt concentrations investigated, the monomer−octamer association is accompanied by positive values of ΔH°_θ and ΔS°_θ, indicating that yTBP assembly is entropy-driven. At low salt ([KCl] ≤ 120 mM), the data are best fit by negative values of $\Delta C^\circ_{p,\theta}$. The combination of positive values of ΔH°_θ and ΔS°_θ and a negative value of $\Delta C^\circ_{p,\theta}$ is often observed for reactions in which large amounts of nonpolar macromolecular surface are removed from water (*43*). However, $\Delta C^\circ_{p,\theta}$ changes with salt concentration. For the monomer−octamer association at 30 °C, the data are most consistent with a large, positive $\Delta C^\circ_{p,\theta}$ at 300 mM KCl and a value near zero at 1 M KCl. In general, the trends observed for the monomer−tetramer and tetramer−octamer reaction steps parallel those of the overall monomer−octamer reaction. With one exception, the monomer−tetramer and tetramer−octamer association reactions are characterized by positive enthalpy and entropy changes (Table 1). Although

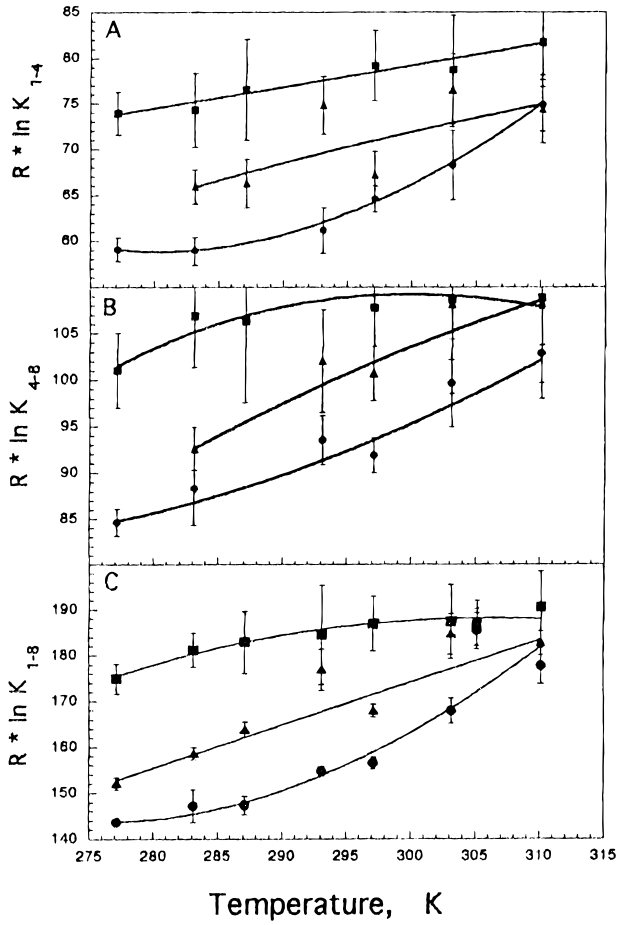

FIGURE 3: Dependence of *S. cerevisiae* TBP self-assembly on temperature. (A) Temperature dependence of R ln K_{obs} for the monomer−tetramer reaction. (B) Temperature dependence of R ln K_{obs} for the tetramer−octamer reaction step. (C) Temperature dependence of R ln K_{obs} for the overall monomer−octamer reaction step. The smooth curves are fits of eq 5 to the data, using $\theta = 303$ K (30 °C). Symbols: (■) 120, (●) 300, and (▲) 1 M KCl. Other reaction conditions are specified in Experimental Procedures.

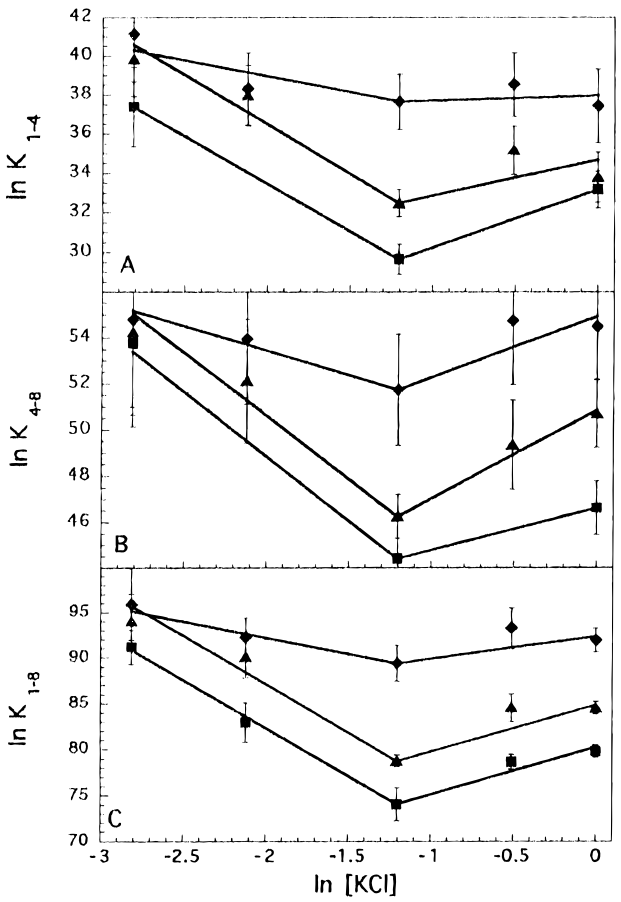

FIGURE 4: Dependence of *S. cerevisiae* TBP self-assembly on KCl concentration. (A) Dependence of ln K_{obs} on ln [KCl] for the monomer−tetramer reaction. (B) Dependence of ln K_{obs} on ln [KCl] for the tetramer−octamer reaction step. (C) Dependence of ln K_{obs} on ln [KCl] for the overall monomer−octamer reaction step. Symbols: (■) 10, (▲) 24, and (◆) 37 °C. Reaction conditions are described in Experimental Procedures.

the experimental uncertainties in $\Delta C^{\circ}_{p,\theta}$ are large, the changes in the most probable values of $\Delta C^{\circ}_{p,\theta}$ with changing salt concentration appear to correlate with shifts in the ionic stoichiometry and with changes in the fluorescence spectrum of the protein (described below). For these reasons, we believe that they reflect changes in the self-association mechanism of the TATA binding protein.

Biphasic Salt Concentration Dependence. The data shown above indicate that the protein stoichiometries of the association reactions are retained over a wide range of [KCl] and temperature. A second feature of interest is the net ionic stoichiometry of each reaction, since this can reveal changes in the number of ionic interactions between protein monomers. A general expression for the self-association of TBP in a buffer in which potassium chloride is the dominant electrolyte is as

$$n\mathrm{TBP} \rightleftarrows \mathrm{TBP}_n + \Delta\nu_{\mathrm{K+Cl}}(\mathrm{K}^+ + \mathrm{Cl}^-) + \Delta\nu_{\mathrm{W}}\mathrm{H_2O} \quad (6)$$

Here $\Delta\nu_{\mathrm{K+Cl}}$ and $\Delta\nu_{\mathrm{W}}$ are the numbers of ions and water molecules released in the assembly reaction, respectively. Note that negative values of $\Delta\nu_{\mathrm{K+Cl}}$ and $\Delta\nu_{\mathrm{W}}$ indicate net *uptake* of ions and water for the reaction as written in eq 6.

The dependence of the apparent association constant of the reaction ($K_{obs} = [\mathrm{TBP}_n]/[\mathrm{TBP}]^n$) is given by (*44*)

$$\frac{\partial \ln K_{\mathrm{obs}}}{\partial \ln[\mathrm{KCl}]} = -\left(\Delta\nu_{\mathrm{K+Cl}} - \frac{2[\mathrm{KCl}]}{55.5}\Delta\nu_{\mathrm{W}}\right) \quad (7)$$

Shown in Figure 4 are representative graphs of ln K_{obs} as functions of ln [KCl] for the monomer−tetramer, tetramer−octamer, and monomer−octamer reaction steps at several of the temperatures analyzed. The most striking features are the biphasic dependences on [KCl], in which values of K_{obs} decrease as [KCl] increases from 60 to 300 mM and then increase as [KCl] increases from 300 mM to 1 M. These results imply that a net *release* of ions accompanies protein oligomerization when [KCl] ≤ 300 mM and that a net *uptake* of ions accompanies oligomerization at [KCl] ≥ 300 mM. This biphasic pattern, described previously for TBP association at a single temperature (*29*), appears to be a general characteristic of yTBP self-association from 4 to 37 °C.

Equation 7 indicates that when salt concentrations are sufficiently low (2[KCl] ≪ 55.5), values of $-\partial \ln K_{obs}/\partial \ln$-[KCl] approximate the numbers of mole equivalents of ions released during a reaction ($\Delta\nu_{\mathrm{K+Cl}}$). This approximation is reasonable unless $|\nu_{\mathrm{W}}| \geq 55.5/2[\mathrm{KCl}]$; the linear dependence of ln K_{obs} on ln[KCl] between 60 and 300 mM KCl and

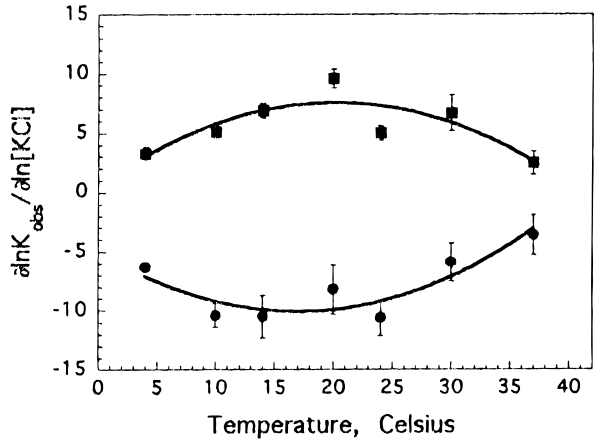

FIGURE 5: Dependence of $\partial \ln K_{obs}/\partial \ln [KCl]$ on temperature for the overall monomer−octamer reaction. Symbols: (●) [KCl] ≤ 300 mM; (■) [KCl] ≥ 300 mM. The near mirror image relationship of these data suggests that the molecular mechanism(s) that give rise to the ion binding events are the same, whether they are probed at high salt or low salt.

between 300 mM and 1 M KCl argues against such large water stoichiometries. (The complete set of values of $\partial \ln K_{obs}/\partial \ln[KCl]$ are presented in Table S1 in Supporting Information.) Relatively large numbers of ions are released during TBP self-association (Figure 5). These large ionic stoichiometries indicate that electrostatic interactions play important roles in the mechanisms of self-association.

Dependence of $\partial \ln K_{obs}/\partial \ln[KCl]$ on Temperature. The net ionic stoichiometries of the monomer−tetramer, tetramer−octamer, and monomer−octamer assembly reactions depend on the reaction temperature. This dependence is biphasic with temperature at both low and high KCl concentrations (Figure 5). For the overall monomer−octamer association, ion stoichiometries reach extreme values near 20 °C, with $\partial \ln K_{obs}/\partial \ln[KCl] \sim -10$ for [KCl] ≤ 300 mM, and $\partial \ln K_{obs}/\partial \ln[KCl] \sim +8$ for KCl] ≥ 300 mM. The ion-linkage stoichiometries of the monomer−tetramer and tetramer−octamer reaction steps have temperature dependences that are less pronounced but nonetheless consistent with the biphasic pattern seen with the monomer−octamer reaction (see Table S1 in Supporting Information). Although the temperature dependence of $\partial \ln K_{obs}/\partial \ln[KCl]$ is weaker for the monomer−tetramer and tetramer−octamer reaction steps, there is no evidence that the ionic stoichiometries of these two reactions diverge with changing temperature. This result is consistent with the notion that similar populations of ion binding sites change occupancy in each reaction step.

Fluorescence Emission Spectra Differ for Monomeric, Tetrameric, and Octameric yTBP. Yeast TBP contains a single tryptophan, located at position 26 (W26) within the 60-residue amino-terminal domain. The fluorescence emission spectrum of this tryptophan is sensitive to changes in TBP oligomerization and to interactions with DNA (*16*). To resolve the spectra of the monomeric, tetrameric, and octameric species, we took advantage of the fact that the centrifuge data identify concentrations in which TBP is predominantly (>98%) monomeric and concentrations in which the protein is predominantly octameric. For example, under our standard buffer conditions, at 120 mM KCl and 30 °C, the monomeric state dominates when $[TBP]_{total} < 1$ μM, and the octameric state dominates when $[TBP]_{total} > 8$ μM (Figure 2D). Fluorescence measurements made under such conditions provide reference spectra for the monomeric and octameric species (Figure 6). These can be used with the mole fractions of monomer (F_M), tetramer (F_T), and octamer (F_O) obtained from parallel sedimentation equilibrium analyses in a linear decomposition of the fluorescence intensities (*45*):

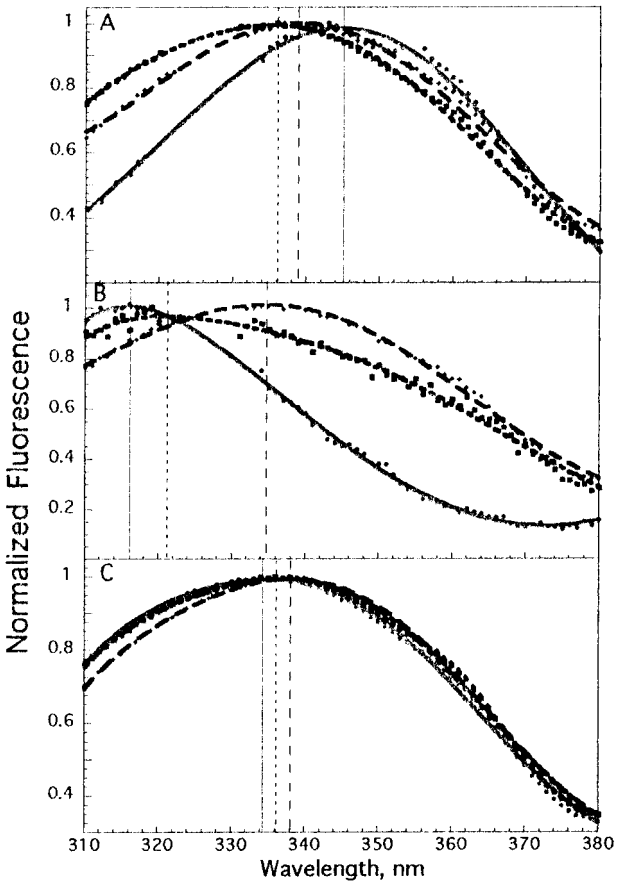

FIGURE 6: Fluorescence emission spectra for the monomeric, tetrameric, and octameric species of yTBP. (A) Spectra of the monomeric species. (B) Spectra of the tetrameric species. (C) Spectra of the octameric species. Spectra for the individual species were obtained as described in the text. The vertical lines represent the fluorescence emission maxima for the individual spectra. Salt concentrations are indicated as follows: solid lines, 60 mM KCl; dotted lines, 120 mM KCl; dashed lines, 600 mM KCl.

$$I_{tot} = F_M I_M + F_T I_T + F_O I_O \quad (8)$$

Here I_{tot}, I_M, I_T, and I_O represent the total fluorescence intensity and the intensities of monomeric, tetrameric, and octameric species, respectively, at a single wavelength. Application of this relationship over a range of wavelengths allowed us to calculate the emission spectrum of the tetramer for representative sets of solution conditions (Figure 6).

The wavelength of maximum fluorescence emission (λ_{max}^{em}) of monomeric TBP ranges from 336 nm (at 300 mM KCl) to 345 nm (at 60 mM KCl). This range is close to the value (348 nm) of tryptophan in water (*39*). The formation of tetramers from monomers is accompanied by a blue shift in the emission maximum. Such a shift is associated with the transfer of the indole chromophore of tryptophan from a polar environment to a less polar one. Of particular interest are the large blue shifts found during tetramerization in

solutions containing 60 and 300 mM KCl. The emission maxima (316 and 321 nm, respectively) are similar to those found for indole dissolved in organic solvents (*46*). This suggests that, in these proteins, W26 is substantially shielded from water. The transition from tetramer to octamer is accompanied by a red shift in the emission spectrum, resulting in values of λ_{max}^{em} near 336 nm. This shift is consistent with an increase in the polarity of the tryptophan environment (*47*). Note that the values of λ_{max}^{em} for tetramer and octamer are smaller than that of the monomer. Since the sum of the mole fractions of tetramer and octamer increase with increasing [TBP] (Figure 2), these results account for the original observation that the fluorescence emission spectrum of TBP shifts toward lower values with increasing protein concentration (*16*).

For each assembly state, changes in KCl concentration are accompanied by significant changes in the emission spectrum. For the monomer, increasing [KCl] from 60 to 300 mM is accompanied by a *decrease* in λ_{max}^{em}, while increasing [KCl] from 300 to 600 mM is accompanied by an *increase* in λ_{max}^{em}. The reversal of the trend of λ_{max}^{em} with [KCl] near 300 mM correlates well with the salt concentration-dependent changes in the ion stoichiometries of TBP association reactions (described in Figure 4). Since the single tryptophan in TBP is located near the middle of the amino-terminal domain sequence, this correlation supports the notion that the amino-terminal domain plays a role in the salt concentration-dependent self-association reaction.

The tetramer displays the greatest salt concentration-dependent change in emission spectrum of any TBP species studied to date. As [KCl] increases from 60 to 300 mM, λ_{max}^{em} increases from 316 to 321 nm. As [KCl] increases from 300 to 600 mM, λ_{max}^{em} increases from 321 to 335 nm. This nearly monotonic increase suggests that the polarity of the environment of W26 increases with increasing [salt]. Evidence that the mobility of this residue also increases with increasing salt (presented below) supports the notion that W26 becomes more solvent-exposed with increasing [KCl].

In contrast to the salt concentration-dependent changes in λ_{max}^{em} seen in the spectra of monomer and tetramer, spectra of the octamer change little with [KCl]. This indicates that the environment of W26 has become relatively insensitive to changes in [salt]. Relatively small changes in fluorescence anisotropy (discussed below) suggest that the mobility of W26 in the octamer is similarly insensitive to [KCl]. The monotonic increase in λ_{max}^{em} with increasing [KCl] suggests that the polarity of the environment of W26 increases with increasing salt concentration. Taken together, these results agree with the original observation (*16*) that the fluorescence emission spectra of the oligomeric states of yeast TBP are blue-shifted as compared to that of the monomeric species.

Values of λ_{max}^{em} Are Temperature Dependent. At 120 mM KCl, λ_{max}^{em} values could be resolved as a function of temperature for the monomeric and octameric forms of yTBP (Figure 7). Reliable temperature-dependent data could not be obtained for the *tetrameric* species because of its small mole fraction (Figure 2) and because this mole fraction is quite strongly temperature dependent. For the octamer, these values are strongly biphasic, decreasing with increasing temperature between 7 and 20 °C and then increasing with temperature between 20 and 40 °C. The reduction of λ_{max}^{em} suggests that W26 may enter an environment of reduced polarity as temperature rises from 7 to 20 °C. At higher temperatures, values of λ_{max}^{em} increase, consistent with a transfer of W26 to an environment of relatively elevated polarity. This increase may reflect thermal denaturation of secondary structure and/or altered tertiary interactions within the amino-terminal domain (*16*). A striking feature of the temperature dependence of λ_{max}^{em} for the octamer is its apparent correlation with the temperature-dependent changes in the net ion stoichiometry for the overall association reaction. The temperature at which the minimum value of λ_{max}^{em} is found (~20 °C) is the same as the temperature that maximizes $\partial \ln K/\partial \ln[KCl]$ when [KCl] ≥ 300 mM and that minimizes $\partial \ln K/\partial \ln[KCl]$ when [KCl] ≤ 300 mM (Figure 5). This coincidence suggests that the amino-terminal domain may change its conformation and/or degree of association with the C-terminal core domain as part of the changes in assembly mechanism revealed by changing ion stoichiometry. For monomeric yTBP at 120 mM KCl, values of λ_{max}^{em} are relatively insensitive to temperature, increasing only slightly at the highest temperatures investigated. This contrasts with the sharp dependence λ_{max}^{em} shown by the octamer and suggests that, in the monomer, the polarity of the environment of W26 is nearly unchanged over the range 2 °C ≤ T ≤ 37 °C.

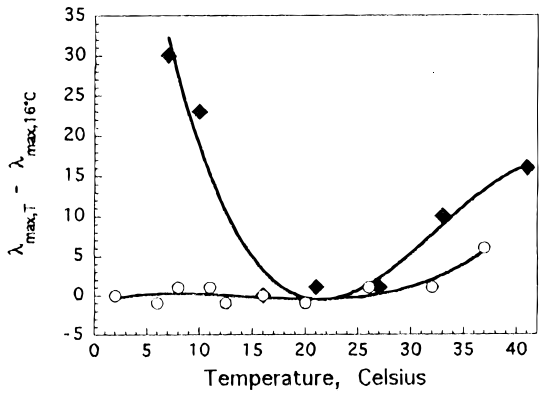

FIGURE 7: Dependence of λ_{max}^{em} on temperature. Symbols: (◆) yTBP octamers; (○) yTBP monomers. The data were obtained in standard buffer containing 120 mM KCl.

Fluorescence Anisotropies Change with Association State and with Increasing [KCl]. When a fluorophore partitions between several states, the fluorescence anisotropy of the ensemble depends on the anisotropy of each state and the mole fraction of each that is present, as described here:

$$r_{tot} = F_M r_M + F_T r_T + F_O r_O \quad (9)$$

Here r_{tot}, r_M, r_T, and r_O represent the total anisotropy and the anisotropies of monomeric, tetrameric, and octameric species, respectively; F_M, F_T, and F_O represent the mole fractions of monomer, tetramer, and octamer present in the sample (cf. refs *48* and *49*). The anisotropies of monomeric and octameric TBP were determined independently, under solution conditions in which these species predominate (see above). The anisotropy of the tetramer could then be calculated by applying eq 9 to the anisotropies of samples containing mixtures of species, with the mole fractions of monomer (F_M), tetramer (F_T), and octamer (F_O) obtained

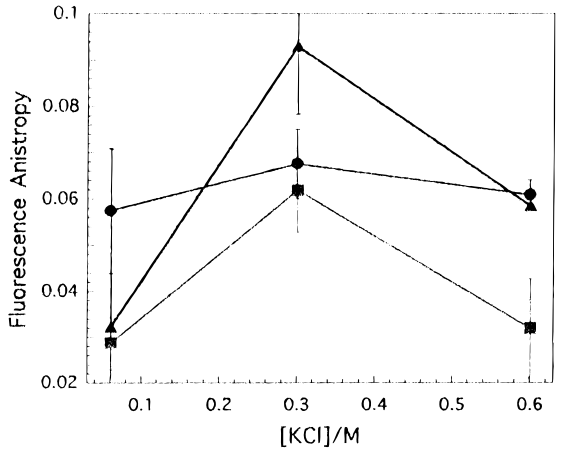

FIGURE 8: Fluorescence anisotropies for the monomeric, tetrameric, and octameric species of yTBP. Symbols: (■) monomer; (▲) tetramer; (●) octamer. Anisotropies for the individual species were obtained by linear decomposition of solution anisotropies as described in the text.

from parallel sedimentation equilibrium analyses. The resulting steady-state anisotropy values (Figure 8) are similar to the limiting values at large sample times of the time-resolved anisotropy of yeast TBP measured by Perez-Howard et al. (*16*). These values are at the low end of the range found in native proteins (*50*), suggesting that the amino-terminal domain is quite mobile on the time scale defined by the excited state of tryptophan 26.

At 60 mM KCl, the formation of octamer from tetramer is accompanied by a significant increase in steady-state anisotropy, but the formation of tetramer from monomer is not. If the excited-state lifetime of tryptophan 26 does not change with oligomerization, this result suggests that the mobility of the tryptophan is reduced on the formation of octamer from tetramer. A different effect is seen at higher salt concentrations. At 300 mM KCl, the formation of tetramer from monomer is accompanied by increased anisotropy, while the formation of octamer from tetramer is accompanied by a reduction of nearly equal amplitude. If the excited-state lifetime of W26 does not change, these results suggest a decrease in mobility on formation of tetramer from monomer and an increase in mobility on formation of octamer from tetramer. Finally, at 600 mM KCl, an increase in anisotropy accompanies the monomer−tetramer transition, but no comparable change is found for the tetramer−octamer transition. This pattern suggests that the mobility of W26 is decreased by monomer−tetramer transition but not affected by the tetramer−octamer step. A striking feature of these results is that the reaction step results in increased anisotropy changes with salt concentration. This observation supports the notion that the mechanism of oligomerization changes with [salt], as proposed above on the basis of changes in ionic stoichiometries.

Finally, it is useful to consider how the fluorescence anisotropy of W26 changes with [KCl] for each assembly state. For monomeric and tetrameric TBP, anisotropy increases between 60 and 300 mM KCl and decreases between 300 and 600 mM KCl. In contrast, the anisotropy of the octameric protein is not significantly affected by changing [KCl] over the experimental range. If the excited-state lifetime of W26 is independent of [KCl], this result suggests that the tryptophan mobilities in monomeric and tetrameric TBP first decrease then increase with increasing [KCl]. Taken with the biphasic dependence of ln K_{obs} on ln[KCl] observed for TBP assembly reactions (Figure 4), these anisotropy results are consistent with models of oligomerization in which the mobilities of the amino-terminal domains are mediated, in part, by ionic interactions.

DISCUSSION

We have examined the self-assembly reactions of yTBP as a function of temperature over the range 4 °C ≤ T ≤ 37 °C and salt concentration over the range 60 mM ≤ KCl ≤ 1 M. Over a very wide range of solution conditions, a monomer−tetramer−octamer association pathway is consistent with the sedimentation equilibrium data. It is also fully consistent with the fluorescence anisotropy decay data of Beechem and co-workers (*16*). TBP association is highly cooperative, with the octameric species favored by ∼9 kcal/mol over the tetrameric species. Accordingly, the tetrameric species is a minor component under all conditions examined, typically not exceeding a mole fraction of 0.2 (Figure 2). In a few cases, the concentrations of tetramer that fit the data were close to zero. In general, this result was found at low temperatures, suggesting that the tetrameric state is disfavored relative to monomer and octamer under these conditions.

Pugh and colleagues have presented data interpreted to indicate that TBP is predominantly dimeric, under native conditions in solution (*26*, *41*). On the basis of their early work and because the C-terminal core domain of yeast TBP crystallizes as a dimer (*25*), we attempted to fit our data with equations that included terms for dimeric TBP. Without exception, these fits were characterized by large, nonrandom residuals and significantly higher values for the square root of the variance than fits with analogous expressions containing only terms for monomer, tetramer, and octamer (results not shown; cf. ref *29*). On this basis, we conclude that our experimental data are not consistent with the presence of a significant population of dimeric TBP. Other evidence that is incompatible with formation of dimers by full-length yeast TBP has been presented, including kinetic and equilibrium DNA binding studies (*16*, *17*) and fluorescence anisotropy decay studies (*16*).

It has been suggested that the absence of dimers in equilibrium experiments might be an artifact of a particular choice of solution conditions (*41*). In the present paper, we have tested a wide range of temperatures and TBP and KCl concentrations as well as representative concentrations of reagents ($MgCl_2$, glycerol, NP-40) that are believed to stabilize the dimer. With the exception of solutions containing detergent, all reaction conditions gave results that were compatible with the monomer−tetramer−octamer association pattern. This outcome emphasizes the robust character of the monomer−tetramer−octamer association pattern and its insensitivity to changes in buffer composition. It has been suggested that TBP monomers might become inactivated for self-association during long incubations such as those necessary for sedimentation equilibrium (*41*). The fact that equilibrium conditions were reliably obtained (and persisted for extended periods during our centrifuge runs) and the observation of DNA binding by yTBP in the ultracentrifuge (M. Daugherty, unpublished results) argue against such

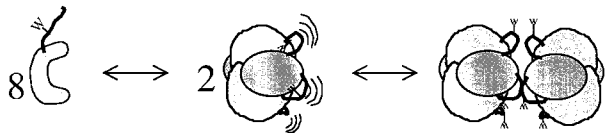

FIGURE 9: Schematic cartoon depicting the change of environment and mobility of tryptophan 26 with oligomerization at low salt concentrations. The amino-terminal domain is represented by the solid line, and the position of the tryptophanyl residue is represented by W. The conserved C-terminal domain is represented by the filled, saddle-shaped figure. Our fluorescence data suggests that W26 shifts from a relatively solvent-exposed environment with relatively high local mobility in the monomer to a more solvent-shielded one of lower mobility in the tetramer and finally to a relatively solvent-exposed environment of yet lower mobility in the octamer. *We emphasize that this scheme represents one of many possible mechanisms of self-association and that the protein surfaces involved in these interactions are currently unknown.*

irreversibility. We suggest that the apparent discrepancy between studies in which dimers are found and those in which they are not reflect differences in the methods used to detect oligomers. The interpretation of nonequilibrium data obtained by chemical cross-linking or GST pull-down techniques is model dependent (indeed, the results of such experiments do not rule out the presence of oligomers above the dimer). On the other hand, quantitative equilibrium techniques such as sedimentation equilibrium and fluorescence anisotropy decay provide rigorous statistical means for distinguishing between competing models.

Conformational Changes Observed for Full-Length Yeast TBP. The resolved fluorescence emission spectra of the monomer, tetramer, and octamer are significantly different, as are the resolved fluorescence anisotropies of these species. These differences suggest that TBP assembly is accompanied by changes in the average conformation and dynamics of the amino-terminal domain. The differences in λ_{max}^{em} at low [salt] are consistent with models in which W26 shifts from a relatively solvent-exposed environment with high local mobility in the monomer to a more solvent-shielded one of lower mobility in the tetramer and finally to a relatively solvent-exposed environment of yet lower mobility in the octamer (Figure 9). These effects are less pronounced at higher [salt], consistent with the notion that ionic interactions determine, in part, the environment of the amino-terminal domain.

At 120 mM KCl, the value of the fluorescence λ_{max}^{em} for the octamer is strongly temperature dependent, going through a minimum near 20 °C. This temperature sensitivity is not observed when the protein is monomeric; increase in λ_{max}^{em} is only seen at the highest temperatures tested (Figure 7). In agreement with this result, Perez-Howard et al. found that monomeric TBP undergoes two thermal transitions, with midpoints at 30 and 42 °C (*16*). We interpret the difference in thermal stability of λ_{max}^{em} as evidence that the interactions that determine the solvent exposure of W26 are stronger in the monomer than in the octamer and do not suffer disruption until relatively high temperatures are reached. This contrast supports models in which the interactions that determine the environment and the dynamics of the amino-terminal domain are qualitatively different in monomer and octamer.

The monomer−tetramer and tetramer−octamer assembly steps are both accompanied by changes in ion stoichiometry and fluorescence properties that depend strongly on [KCl]. Both reaction steps are accompanied by net ion release when [KCl] ≤ 300 mM, while net ion uptake is observed for both at higher salt concentrations. The magnitude of the blue shift in the fluorescence λ_{max}^{em} that accompanies the formation of tetramers from monomers is strongly salt concentration-dependent, as is the magnitude of the red shift in λ_{max}^{em} that accompanies octamer formation from tetramers. In addition, the association step in which the fluorescence anisotropy undergoes its greatest increase switches from the tetramer−octamer step at low [salt] to the monomer−tetramer step at high [salt]. Finally, the standard heat capacity differences that accompany assembly of monomers to octamers are strongly biphasic with [KCl], ranging from -2.2 ± 3.6 kcal mol^{-1} K^{-1} at 60 mM KCl to 4.6 ± 1.2 kcal mol^{-1} K^{-1} at 300 mM KCl to 0.1 ± 1.2 kcal mol^{-1} K^{-1} at 1 M KCl. Taken together, these results suggest that the mechanism(s) of full-length yTBP self-assembly undergo a concerted salt concentration-dependent switch near 300 mM KCl.

What is the Nature of the Switch? Since the sedimentation equilibrium data rule out changes in protein stoichiometry, the changes in ion stoichiometry and fluorescence must correspond to alteration(s) in the conformation of the protein and/or the identity of the interacting surfaces. Intriguingly, values of $\partial \ln K_{obs}/\partial \ln[KCl]$ for the monomer−tetramer reaction are similar in sign and magnitude to those for the tetramer−octamer step (Figure 4; see also Table S1 in Supporting Information). Although it seems unlikely that the protein surfaces that interact to form the tetramer could be identical to those that interact to form the octamer, similar populations of ion-binding sites may participate in both assembly reactions. The similar trends of $\ln K_{obs}$ with ln-[KCl] for monomer−tetramer and tetramer−octamer reactions support the notion that the ionic interactions accompanying these reaction steps are sensitive to the same changes in protein structure, whether they are observed at low [salt] (with net ion release) or high salt (with net ion uptake).

The fluorescence data suggests that in the monomeric species, the environment of W26 becomes solvent-exposed and slightly more mobile with salt concentration. In contrast, for the tetrameric species, the fluorescence data suggest that the environment of W26 becomes more solvent-exposed but less mobile with salt concentration. Finally, for the octamer, neither the value of λ_{max}^{em} nor the anisotropy are greatly [salt]-dependent, consistent with models of the octamer in which the environment of the amino-terminal domain is not constrained by ionic interactions susceptible to disruption by changes in [KCl] between 60 mM and 1 M. These results suggest that salt concentration-dependent conformational changes in monomer and tetramer alter the self-association mechanisms of TBP. Comparison of the crystal structures of yeast TBP C-terminal domain dimer and the complex of the C-terminal domain with TATA DNA reveals only minor conformational differences (*13*), and similar data has been presented for crystalline dimeric and DNA-bound forms of TBP2 from arabidopsis thaliana (*15*). These results suggest that the C-terminal core domain is a highly rigid structure. We therefore propose that the conformational changes detected by fluorescence and ionic stoichiometry differences are largely confined to the amino-terminal domain.

Ionic Linkage to DNA Binding. At 30 °C and pH 7.4, the binding of full-length yeast TBP to the adenovirus E4

promoter TATA sequence is accompanied by the net release of 3.6 ± 0.3 mole equiv of monovalent ions (*18*). Under closely similar reaction conditions, the dissociation of tetramer to monomers is accompanied by a net uptake of 3.3 ± 1.3 mole-equivalent of monovalent ions, and the dissociation of octamer to monomers is accompanied by a net uptake of 5.9 ± 1.6 mole-equivalent (Figure 4; see also Table S1 in Supporting Information). In each case, this is equivalent to a net uptake of ~0.75 ion equivalent per TBP monomer dissociated. Coupling of dissociation of tetrameric or octameric TBP to DNA binding should effectively reduce the number of ions released by ~0.75 per TBP−TATA complex formed. This reduction in the net ion stoichiometry significantly diminishes the salt concentration dependence of the affinity of TBP for TATA DNA and might help to protect TBP−DNA interactions from any change in intracellular salt concentration.

Possible Sources of Entropy. The assembly reactions of TBP are entropy-dominated under all KCl concentrations studied (Table 1). Potential contributors to the large, positive values of $\Delta S°$ that accompany oligomerization include changes in the entropy of the protein, changes in solvent entropy, and changes in the entropies of ions participating in the reaction. Although it is clear that oligomerization should reduce the translational and rotational entropies of TBP monomers, our data do not rule out an increase in the conformational entropy of monomers accompanying association. The changes in fluorescence emission wavelength and anisotropy that accompany oligomerization are consistent with models in which the amino-terminal domain changes conformation and mobility at each step in the reaction. Such changes contribute to the conformational entropy of the system. Net ion release might also contribute to positive values of $\Delta S°$ but only at low salt concentrations, since the assembly reactions are accompanied by net ion uptake at all values of [KCl] > 300 mM (Figure 4). Water release from interacting surfaces has been identified as an important contributor to $\Delta S°$ (*51*). We anticipate that the surfaces that interact in formation of tetrameric and octameric TBP species are large. If this is the case, water release may be the dominant contributor to $\Delta S°$.

Are Tetramers and Octamers Physiologically Relevant? The distribution of the mole fractions of monomers, tetramers, and octamers at equilibrium under approximately physiological conditions of temperature and salt concentration (30 °C, 120 mM KCl) are shown in Figure 2D. A striking feature of this distribution is that the octameric species is the predominant form of full-length yTBP at the concentration estimated to occur in the yeast nucleus (~6.3 μM (*29*)). This species distribution refers to a solution that contains only TBP at the indicated temperature and salt concentration. Although evidence has been presented for the oligomerization of yTBP in vivo (*52*), it remains to be discovered whether the oligomers are tetramers and/or octamers.

It has been estimated that there are 30 000−50 000 TBP molecules per yeast cell (*53*). If the form of TBP that is active in transcription regulation is the monomer, as suggested by many authors (*13*−*18*), and if each of the ~6000 promoters (*54*) present in the yeast genome binds a molecule of TBP, then at least 24 000 molecules of TBP remain to engage in other interactions. This corresponds to a TBP concentration of ~5.2−5.7 μM (Figure 2, closed arrows). Under approximately physiological buffer conditions, but in the absence of other interactions, the octamer remains the dominant form of TBP in this concentration range. It is well-known that TBP interacts with many proteins including TAFs, transcription factors (including Mot1, NC2, Nots, and SAGA (*53*)), proteins of the nuclear pore complex (*55*), and transport factors (*56*); these interactions are expected to significantly reduce the concentration of free TBP. However, we emphasize that if any TBP is present as free protein, all hetero-interactions (including transcription regulatory ones) must compete with TBP's tendency to self-associate.

What Cellular Functions Might Be Fulfilled by TBP Oligomerization? Self-association may control the availability of yTBP monomers for interaction with DNA. Yeast TBP monomers bind DNA with relatively low sequence specificity, and TBP is capable of nucleating the assembly of functional transcription−initiation complexes at nonspecific sites (*26*). Limiting the availability of monomeric TBP may minimize promiscuous DNA binding by this species. Alternately, it is possible that DNA binding by TBP oligomers (as visualized by Griffith et al. (*57*)) may play a role in transcription regulation. Self-association may control the availability of TBP monomers for interaction with transcription factors and TAFs. TBP interacts stably with different populations of proteins in polymerase I, II, and III transcription−initiation complexes (*1*, *53*). Self-associated TBP may act as a reservoir of uncommitted protein, allowing rapid changes in the balance of polymerase I, II, and III activities. Kinetic studies show that the rate of DNA binding is not limited by the self-association of yTBP to tetramers and octamers (*35*), consistent with the notion that yTBP oligomers provide a supply of protein that can be quickly made available for cellular processes. In addition, the availability of competing self-interaction modes may facilitate the switching of TBP between different ensembles of regulatory interactions. TBP oligomerization may limit its transport across the nuclear envelope. Recently Pemberton and colleagues have discovered a protein complex (Kap114p) that transports TBP across the nuclear membrane (*58*). It seems possible that oligomerization may limit the functional interactions of TBP with this machinery. Monomeric TBP (M_r = 27 018) may be small enough for passive diffusion through nuclear pore complexes, which limit passive transport to proteins smaller than $M_r \sim 40\,000$ (*59*). On the other hand, tetramers (M_r = 108 072) and octamers (M_r = 216 864) are significantly larger than this limit. Oligomerization may represent a mechanism for maintaining a concentration gradient of TBP across the nuclear envelope. Finally, TBP oligomerization may protect the protein from inactivation. Pugh and colleagues have demonstrated a correlation between oligomer stability and the steady-state expression level of yTBP in vivo (*52*). They interpret this result as evidence that TBP−TBP interactions stabilize the protein against degradation. Limiting the turnover of TBP might ensure the availability of active protein to respond to changes in gene regulatory stimuli.

Different Association Mechanisms for Full-Length and Core yTBPs. Two features of our data indicate that the mechanisms of full-length yTBP oligomerization involve different protein surfaces than are utilized for formation of the crystalline dimer structures. First, our data are incompat-

ible with the presence of a significant mole fraction of TBP dimer at any temperature or salt concentration in the range 4 °C ≤ T ≤ 37 °C and 60 mM ≤ [KCl] ≤ 1 M. On the other hand, the crystallization of the C-terminal core domain as a dimer as well as solution light-scattering data (*31*) indicate that the dimer is a stable species of core TBP. The contrast between the self-association modes of core and full-length yTBP is consistent with the notion that the amino-terminal domain influences the assembly mechanism. Second, the changes in fluorescence λ_{max}^{em} and steady-state anisotropy described in this paper indicate that the region of the amino-terminal domain near W26 undergoes significant changes in solvent exposure and mobility during tetramer and octamer formation (Figure 9). Clearly, the formation of dimers by the C-terminal core cannot involve these residues.

CONCLUSIONS

These studies show that the conformations of full-length yeast TBP and its mechanisms of self-association undergo dramatic changes as functions of temperature and [KCl]. Despite these mechanistic and structural changes, the overall association pattern is surprisingly robust, remaining monomer−tetramer−octamer over a wide range of solution conditions. Taken together with previous evidence that the C-terminal domain can form stable dimers in solution and in crystals (*31*), these results imply a significant plasticity in the structure of TBP that is likely to play important roles in its quaternary interactions.

SUPPORTING INFORMATION AVAILABLE

A table giving the ionic linkage stoichiometries of the monomer−tetramer, tetramer−octamer, and monomer−octamer association reactions of full-length yTBP, determined at temperatures ranging from 4 to 37 °C (1 page). This material is available free of charge via the Internet at http://pubs.acs.org.

REFERENCES

1. Goodrich, J. A., and Tjian, R. (1994) *Curr. Opin. Cell Biol. 6*, 403−409.
2. Verrijzer, C. P., and Tjian, R. (1996) *Trends Biochem. Sci. 21*, 338−342.
3. Hahn, S., Buratowski, S., Sharp, P. A., and Guarente, L. (1989) *Proc. Natl. Acad. Sci. U.S.A. 86*, 5718−5722.
4. Peterson, M. B., Tanese, N., Pugh, B. F., and Tjian, R. (1990) *Science 248*, 1625−1630.
5. Buratowski, S., Hahn, S., Guarente, L., and Sharp, P. A. (1989) *Cell 56*, 549−561.
6. Maldonado, E., Ha, I., Cortes, P., Weis, L., and Reinberg, D. (1990) *Mol. Cell. Biol. 10*, 6335−6347.
7. Van Dyke, M. W., Roeder, R. G., and Sawadogo, M. (1988) *Science 241*, 1335−1338.
8. Pugh, B. F., and Tjian, R. (1991) *Genes Dev. 5*, 1935−1945.
9. Cormack, B. P., and Struhl, K. (1992) *Cell 69*, 685−696.
10. White, R. J., and Jackson, S. P. (1992) *Trends Genet. 8*, 284−288.
11. Struhl, K. (1994) *Science 263*, 1103−1104.
12. Schultz, M. C., Reeder, R. H., and Hahn, S. (1992) *Cell 69*, 697−702.
13. Kim, J. L., and Burley, S. K. (1994) *Nat. Struct. Biol. 1*, 638−653.
14. Kim, J. L., Nikolov, D. B., and Burley, S. K. (1993) *Nature 365*, 520−527.
15. Kim, Y., Geiger, J. H., Hahn, S., and Sigler, P. B. (1993) *Nature 365*, 512−520.
16. Perez-Howard, G. M., Weil, P. A., and Beechem, J. M. (1995) *Biochemistry 34*, 8005−8017.
17. Parkhurst, K. M., Brenowitz, M., and Parkhurst, L. J. (1996) *Biochemistry 35*, 7459−7465.
18. Petri, V., Hsieh, M., and Brenowitz, M. (1995) *Biochemistry 34*, 9977−9984.
19. Rudloff, U., Eberhard, D., and Grummt, I. (1994) *Proc. Natl. Acad. Sci. U.S.A. 91*, 8229−8233.
20. Zawel, L., and Reinberg, D. (1995) *Annu. Rev. Biochem. 64*, 533−561.
21. Zhou, Q., and Berk, A. J. (1995) *Mol. Cell. Biol. 15*, 534−539.
22. Nikolov, D. B., Chen, H., Halay, E. D., Usheva, A. A., Hisatake, K., Lee, D. K., Roeder, R. G., and Burley, S. K. (1995) *Nature 377*, 119−128.
23. Lee, D. K., DeJong, J., Hashimoto, S., Horikoshi, M., and Roeder, R. G. (1992) *Mol. Cell. Biol. 12*, 5189−5196.
24. Nikolov, D. B., Hu, S.-H., Lin, J., Gasch, A., Hoffman, A., Horikoshi, M., Chua, N.-H., Roeder, R. G., and Burley, S. K. (1992) *Nature 360*, 40−46.
25. Chasman, D. I., Flaherty, K. M., Sharp, P. A., and Kornberg, R. D. (1993) *Proc. Natl. Acad. Sci. U.S.A. 90*, 8174−8178.
26. Coleman, R. A., Taggart, A. K. P., Benjamin, L. R., and Pugh, B. F. (1995) *J. Biol. Chem. 270*, 13842−13849.
27. Kato, K., Makino, Y., Kishimoto, T., Yamauchi, J., Kato, S., Muramatsu, M., and Tamura, T.-a. (1994) *Nucleic Acids Res. 22*, 1179−1185.
28. Oberleithner, H., Schneider, S., and Bustamante, J.-O. (1996) *Pflugers Arch−Eur. J. Phys. 432*, 839−844.
29. Daugherty, M. A., Brenowitz, M., and Fried, M. G. (1999) *J. Mol. Biol. 285*, 1389−1399.
30. Coleman, R. A., and Pugh, B. F. (1997) *Proc. Natl. Acad. Sci. U.S.A. 94*, 7221−7226.
31. Nikolov, D. B., and Burley, S. K. (1994) *Nat. Struct. Biol. 1*, 621−637.
32. O'Brien, R., DeDecker, B., Fleming, K. G., Sigler, P. B., and Ladbury, J. E. (1998) *J. Mol. Biol. 279*, 117−125.
33. Icard-Liepkalns, C. (1993) *Biochem. Biophys. Res. Commun. 193*, 453−459.
34. Petri, V., Hsieh, M., Jamison, E., and Brenowitz, M. (1998) Personal communication.
35. Parkhurst, K. M., Richards, R. M., Brenowitz, M., and Parkhurst, L. J. (1999) *J. Mol. Biol. 289*, 1327−1341.
36. Mohan, C. (1997) *Buffers: A Guide for the Preparation and Use of Buffers in Biological Systems*, Calbiochem-Novabiochem Corporation, La Jolla, CA.
37. Cohn, E. J., and Edsall, J. T. (1943) *Proteins, Amino Acids and Peptides as Ions and Dipolar Ions*, Reinhold, New York.
38. McRorie, D. K., and Voelker, P. J. (1993) *Self-Associating Systems in the Analytical Ultracentrifuge*, Beckman Instruments, Inc., Palo Alto, CA.
39. Johnson, M. L., Correia, J. J., Yphantis, D. A., and Halvorson, H. R. (1981) *Biophys. J. 36*, 575−588.
40. Lakowicz, J. R. (1983) *Priciples of Fluorescence Spectroscopy*, Plenum Press, New York.
41. Jackson-Fisher, A. J., Burma, S., Portnoy, M., Schneeweis, L. A., Coleman, R. A., Mitra, M., Chitikila, C., and Pugh, B. F. (1999) *Biochemistry 38*, 11340−11348.
42. Clarke, E. C. W., and Glew, D. N. (1966) *Trans. Faraday Soc. 62*, 539−547.
43. Spolar, R. S., Ha, J. H., and Record, M. T., Jr. (1989) *Proc. Natl. Acad. Sci. U.S.A. 86*, 8382−8385.
44. Record, M. T., Jr., Ha, J. H., and Fisher, M. A. (1991) *Methods Enzymol. 208*, 291−343.
45. Cantor, C. R., and Schimmel, P. S. (1980) *Biophysical Chemistry Part II: Techniques for the study of biological structure and function*, W. H. Freeman and Company, New York.
46. Konev, S. V. (1967) *Fluorescence and Phosphorescence of Proteins and Nucleic Acids*, Plenum Press, New York.
47. Lakowitz, J. R. (1983) *Principles of Fluorescence Spectroscopy*, pp 342−381, Plenum Press, New York.

48. Rajkowski, K. M., and Cittanova, N. (1981) *J. Theor. Biol. 93*, 691−696.
49. Lundblad, J. R., Laurance, M., and Goodman, R. H. (1996) *Mol. Endocrinol. 10*, 607−612.
50. Beechem, J. M., and Brand, L. (1985) *Annu. Rev. Biochem.* 43−71.
51. Parsegian, V. A., Rand, R. P., and Rau, D. C. (1995) *Methods Enzymol. 259*, 43−94.
52. Jackson-Fisher, A. J., Chitikila, C., Mitra, M., and Pugh, B. F. (1999) *Mol. Cell 3*, 717−727.
53. Lee, T. I., and Young, R. A. (1998) *Genes Dev. 12*, 1398−1408.
54. Goffeau, A., Barrell, B. G., Bussey, H., Davis, R. W., Dujon, B., Feldmann, H., Galibert, F., Hoheisel, J. D., Jacq, C., Johnston, M., Louis, E. J., Mewes, H. W., Murakami, Y., Philippsen, P., Tettelin, H., and Oliver, G. G. (1996) *Science 274*, 546−567.
55. Bustamante, J. O., Liepins, A., Prendergast, R. A., Hanover, J. A., and Oberleithner, H. (1995) *J. Membr. Biol. 146*, 263−272.
56. Pemberton, L. F., Rosenblum, J. S., and Blobel, G. (1999) *J. Cell Biol. 145*, 1407−1417.
57. Griffith, J. D., Makhov, A., Zawel, L., and Reinberg, D. (1995) *J. Mol. Biol. 246*, 576−584.
58. Pemberton, L. F., Rosenblum, J. S., and Blobel, G. (1999) *J. Cell Biol. 145*, 1407−1417.
59. Miller, M., Park, M. K., and Hanover, J. A. (1991) *Phys. Rev. 71*, 909−949.

BI992423N